Pressure effects on the electronic properties and superconductivity of the β-pyrochlore oxides: $A\mathrm{Os_2O_6}$ (A=Na, K, Rb, Cs)

R. Saniz and A. J. Freeman
Department of Physics and Astronomy, Northwestern University, Evanston, Illinois 60208-3112, USA
(Received 14 February 2005; revised manuscript received 17 May 2005; published 15 July 2005)

We present a first-principles study of the electronic structure and superconducting parameters of the compounds $A\mathrm{Os_2O_6}$ (A=Na, K, Rb, and Cs) and at ambient and applied hydrostatic pressure. We find that the sensitivity of the density of states at the Fermi energy, E_F, and related electronic properties to the size of the alkali metal atom as well as to applied pressure is driven by a van Hove singularity with energy very close to E_F. Further, a computation of the superconducting parameters of these materials allows us to show that the observed change of T_c, both upon substitution of the alkali metal and under applied hydrostatic pressure, can be well understood within a phonon-mediated pairing scenario. In this regard, we find that the correction to the effective electron mass due to spin fluctuations plays a significant role.

DOI: 10.1103/PhysRevB.72.024522 PACS number(s): 74.70.Dd, 71.20.Be, 74.25.Jb

I. INTRODUCTION

During the last decade or so, the search and interest in the superconductivity of non-Cu-based oxides has extended from an effort to understand the pairing mechanism in the cuprates to a broader search of superconductivity in materials in which electron correlations are thought to play a determining role. To this end, researchers try to exploit a diverse range of factors, from the orbital degrees of freedom to the crystal structure of the material. A particularly interesting example is the recently discovered family of superconducting Os-oxide β-pyrochlores $A\mathrm{Os_2O_6}$, with A=K, Rb, and Cs,[1–3] which have superconducting transition temperatures T_c=9.6 K, 6.3 K, and 3.3 K, respectively. The pyrochlore structure is a network of corner sharing tetrahedra and is a geometrically frustrated spin system if the ions bear a localized magnetic moment interacting antiferromagnetically with their nearest neighbors. Further, the Os ions—located at the tetrahedra vertices—possess a formal oxidation state of 5.5 + ($5d^{2.5}$). As pointed out by Hiroi and co-workers,[4] compared to other transition metal pyrochlore oxides, this places these materials between $\mathrm{Cd_2Re_2O_7}$ ($\mathrm{Re^{5+}}$:$5d^2$), which is a good conductor at low temperatures (becoming a superconductor at $\sim$1 K)[5,6] and $\mathrm{Cd_2Os_2O_7}$ ($\mathrm{Os^{5+}}$:$5d^3$), which is an insulator at low temperatures and exhibits antiferromagnetic ordering.[7]

While the several experimental results[1–3,8–13] reported during the past year provide key information, the pairing mechanism in these materials is still under debate. These experiments indicate similarities but also differences among the compounds with different alkali metal, tending to single out $\mathrm{KOs_2O_6}$. Let us mention briefly some of the observations that should be taken into account by any proposed pairing mechanism. First, the very change in T_c upon substitution of the alkali atom (A) may be initially counterintuitive. Indeed, the negative chemical pressure leads to an increase of the lattice constant with the ionic radius of A, so that one may expect T_c to increase because band narrowing should lead to an increase of the density of states (DOS) at the Fermi level (E_F). As shown by the reported T_c's above, however, the opposite occurs. In line with these findings, the change in T_c under applied hydrostatic pressure is found to be initially positive in all of these materials.[12,13] This has been interpreted as suggesting that the pairing mechanism in these materials is unconventional, or non-BCS-like.[3] Of interest is the fact that in $\mathrm{KOs_2O_6}$ the increase of T_c with pressure reaches a maximum at 0.56 GPa and tends to vanish gradually at higher pressures.[13,14]

Further observations are that the temperature dependence of the resistivity shows an unusual concave behavior at low temperature in the case of $\mathrm{KOs_2O_6}$,[1] while a T^2 behavior is observed[2] just above T_c in the case of $\mathrm{RbOs_2O_6}$, and on a larger temperature interval[3] in the case of $\mathrm{CsOs_2O_6}$. Also, nuclear magnetic resonance experiments reveal a weak temperature dependence of the Knight shift of both the ^{39}K and ^{87}Rb nuclei in the corresponding pyrochlores.[9,10] In the normal state, however, the relaxation rate divided by temperature ($1/TT_1$) follows the Korringa relaxation in the case of Rb,[9] or deviates weakly from it,[10] but deviates more strongly from this behavior in the case of K.[10] In both cases, however, there appears to be evidence for antiferromagnetic spin fluctuations. Finally, regarding the superconducting gap, Magishi and co-workers[9] find that the relaxation rate in the superconducting state suggests an anisotropic but nodeless gap in $\mathrm{RbOs_2O_6}$; at the same time, Koda and collaborators[11] interpret their muon spin rotation study of the magnetic penetration depth in $\mathrm{KOs_2O_6}$ as pointing to an anisotropic gap with nodes.[11]

We report here on a first-principles study of the electronic structure and superconducting parameters of the compounds $A\mathrm{Os_2O_6}$ (A=Na, K, Rb, and Cs) and on the effects of hydrostatic pressure. We find that the main traits of the electronic structure reported previously[15] in the case of $\mathrm{KOs_2O_6}$ are common to all of these materials, with relatively small qualitative and quantitative changes. The differences essentially stem from the energy level with respect to E_F of the van Hove singularity (vHS) with momentum $\mathbf{k}$ near the center of the Γ-L line. In particular, the DOS at the Fermi energy, $N(E_F)$, tends to increase with the size of A because the vHS is pushed closer to E_F. The effect of applied hydrostatic pres-

TABLE I. Structural parameters of the Os-oxide β-pyrochlores within the GGA approximation ($T=0$ K).

Compound	a (Å)	x	$l_{\mathrm{Os-O}}$ (Å)	∠O–Os–O	∠Os–O–Os	B (GPa)
$NaOs_2O_6$	10.274	0.317	1.942	88.26	138.57	113.9
KOs_2O_6	10.298	0.316	1.944	88.54	138.98	116.6
$RbOs_2O_6$	10.318	0.315	1.945	88.82	139.39	118.8
$CsOs_2O_6$	10.356	0.314	1.948	89.27	140.03	123.8

sure is to push the vHS away from E_F. This is very clearly reflected by the increase or suppression of a constriction between the two Γ-point centered Fermi surface shells, basically due to a bending of the outer shell that depends on the proximity of the vHS to E_F.

We further estimate T_c with the well-known McMillan–Allen–Dynes expression,[16] with the electron-phonon coupling constant calculated within the crude rigid muffin-tin approximation (RMTA).[17,18] We also calculate the Stoner susceptibility enhancement parameter and estimate the electron-spin coupling constant within the Doniach–Engelsberg approximation.[19] This allows us to show that spin fluctuations contribute importantly to the effective electron mass, significantly reducing T_c. Despite the approximations implicit in these calculations, we find, remarkably, that the calculated T_c follows rather well the trends observed in experiment, both upon substitution of the alkali metal and under hydrostatic pressure. Our results, thus, bring further support to the electron-phonon coupling description of these superconductors.[8,9,12,15]

Section II is devoted to the methodology of our calculations as well as to structural properties; in Sec. III, we present and discuss our results in relation to the experimental findings mentioned above.

II. METHODOLOGY AND STRUCTURAL ASPECTS

We use the highly precise full-potential linearized augmented plane-wave[20] implementation of the density functional approach to the electronic structure and properties of crystalline solids. We make our self-consistent calculations within the Perdew, Burke, and Ernzerhof generalized gradient approximation (GGA) (Ref. 21) to the exchange-correlation potential and include the spin-orbit coupling (SOC) term in the Hamiltonian. Angular momenta up to $l=8$ are used for both the charge density in the muffin tins and the wave functions. The irreducible part of the Brillouin zone is sampled with a uniform mesh of 120 **k** points. The Os $5p$ and K $3p$ states are treated as valence electrons.

The β-pyrochlores crystallize in a cubic structure with space group $Fd\bar{3}m$. There are 18 atoms in the unit cell: Two A atoms ($8b$), four Os atoms ($16c$), and twelve O atoms ($48f$). The Os atoms are octahedrally coordinated by six O atoms. An internal parameter, x, fixes the positions of the latter and thereby also determines the degree of rhombohedral distortion of the octahedra enclosing the Os atoms. In all the cases considered, we determine the lattice constant, a, as well as x, by minimizing the total energy and ensuring that the total force on the O atoms is less than 10^{-4} a.u. The muffin-tin radii used are 2.2 a.u. for the Os ions and 1.3 a.u. for the O ions. The corresponding values for the Na, K, Rb, and Cs ions are, respectively, 2.6, 2.8, 3.0, and 3.1 a.u.

The values of the calculated structural parameters are reported in Table I, including the smaller Os—O—Os angle defining the main rectangular cross section of the octahedra and the O—Os—O angle characterizing the staggered Os—O chains on the underlying the pyrochlore lattice. The calculated ($T=0$ K) lattice constants differ from the (room temperature) experimental results of Hiroi and co-workers (see Ref. 13) by +1.95% for KOs_2O_6, +1.98% for $RbOs_2O_6$, and +2.00% for $CsOs_2O_6$. Although the compound with Na has not been synthesized—probably because of its small size—we have included it in our study to better identify the trends followed by the different properties upon A substitution. With respect to the other parameters in Table I, unfortunately, the only experimental values reported are those of Brühwiler *et al.*[8] for $RbOs_2O_6$. In this case, the difference of the calculated Os—O bond length from experiment is +1.8%, while the difference for the internal parameter, and the O—Os—O and Os—O—Os angles are, notably, all below 0.1%. From Table I, it is clear that the angle in the Os—O chains increases with decreasing T_c. Assuming a phonon mediating pairing, it was suggested[8] that this angle plays a role in determining T_c. Future studies of the phonon spectra of these materials should allow one to verify this interesting point. In Table I, we also give the calculated bulk moduli, which are necessary to calculate volume changes under pressure.

III. ELECTRONIC STRUCTURE AND PROPERTIES

A. Band structure and density of states

As we reported previously in the case of KOs_2O_6,[15] we find that in all the β-pyrochlores the band structure around E_F is given by a manifold of 12 bands arising mainly from Os $5d$ states and O $2p$ states. The dispersion of the bands is generally the same for the different compounds, but there is an important difference near E_F, which is that the vHS near the center of the Γ-L line moves up closer to the Fermi level as the size of A increases. This is clearly illustrated in Fig. 1, where we compare the energy bands of the different compounds for **k** points along the Γ-L. The consequence of this for DOS is also intriguing. Indeed, although the peak due to the vHS tends to decrease for the cases with a larger A ion, $N(E_F)$ increases because the vHS is closer to E_F. This is clear from Fig. 2, where we show a close-up of the total DOS around E_F for the different compounds. In Table II, where we list the total DOS at E_F, as well as the muffin-tin sphere

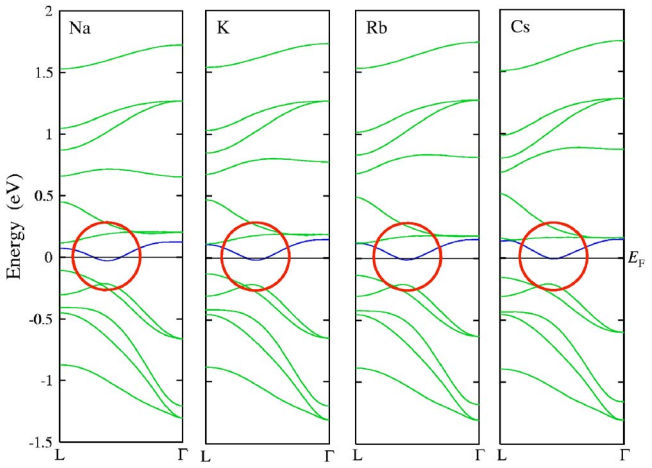

FIG. 1. (Color online) The manifold of 12 energy bands near E_F of the superconducting β-pyrochlore Os oxides plotted for **k** points along the L-Γ line. The band crossing E_F is highlighted in blue, and the red circle indicates the location of the van Hove singularity. It is clearly seen that the larger the alkali metal, the closer the singularity is to E_F.

projected DOS for O and Os. For reference, we also indicate the values of the bare band Sommerfeld coefficient and of the band Pauli paramagnetic susceptibility. Comparing with measurements on powder samples, the specific heat mass-enhancements, $\gamma_{\mathrm{exp}}/\gamma_b$, appear to be 3.3 for KOs_2O_6 ($\gamma_{\mathrm{exp}}=19$ mJ/K^2 mol Os) (Ref. 4) and 3.7 for $RbOs_2O_6$ ($\gamma_{\mathrm{exp}}=44$ mJ/K^2 mol Os).[22] If the results reported by Muramatsu *et al.*[13] are used for $RbOs_2O_6$ and $CsOs_2O_6$ (both with $\gamma \simeq 20$ mJ/K^2 mol Os), one finds mass enhancements of 3.4 and 3.2, respectively. We note, however, that very recently

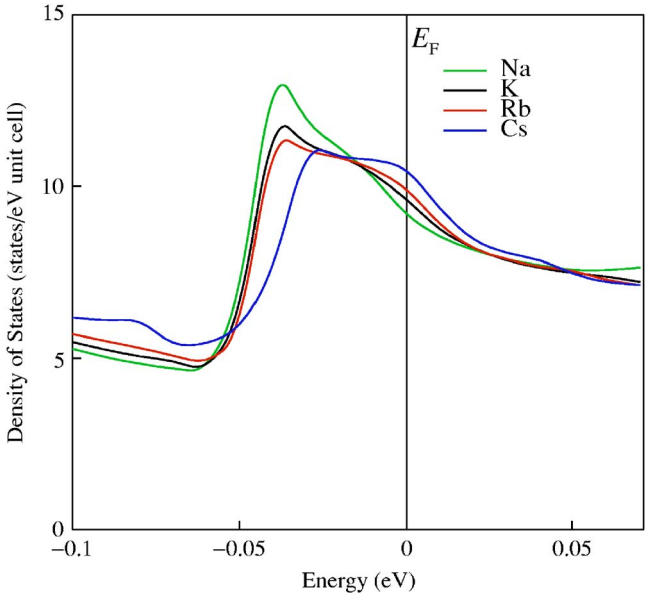

FIG. 2. (Color online) Density of states at E_F for the β-pyrochlore Os oxides. Although the height of the van Hove peak itself tends to decrease with the size the alkali ion, the value of $N(E_F)$ increases because the singularity shifts up in energy toward E_F.

TABLE II. Total DOS (states/eV unit cell) and muffin-tin sphere projected DOS (states/eV atom) at E_F. Also given are the bare band Sommerfeld coefficient (mJ/K^2 mol$_{\mathrm{f.u.}}$) and the band Pauli paramagnetic susceptibility ($\times 10^6$).

	$NaOs_2O_6$	KOs_2O_6	$RbOs_2O_6$	$CsOs_2O_6$
Total	9.13	9.64	9.96	10.58
A	0.019	0.020	0.030	0.048
Os	4.542	4.783	4.927	5.191
O	2.578	2.751	2.864	3.070
γ_b	10.76	11.36	11.74	12.46
χ_b	1.81	1.90	1.95	2.04

Hiroi and co-workers[23] reported specific heat measurements on a single crystal sample of KOs_2O_6, which, making an estimate similar to the powder sample case, yields a surprising $\gamma_{\mathrm{exp}}=64.8$ mJ/K^2 mol Os. This results in an unusually large $\gamma_{\mathrm{exp}}/\gamma_b \simeq 11.4$.[24]

The effect of hydrostatic pressure is basically to push the eigenvalues around E_F downward. We illustrate this in the case of $RbOs_2O_6$ in Fig. 3, where we show a close look at the bands around E_F both for a sample under zero pressure and a sample under simulated pressure such that the change in the lattice constant is $\Delta a/a=-2\%$. While this corresponds to a relatively large pressure, it clearly shows the effect on the vHS, pushing it away from E_F. This naturally leads to a decrease of $N(E_F)$. As a further quantitative illustration, in Table III we list $N(E_F)$ for various pressures in the case of KOs_2O_6.

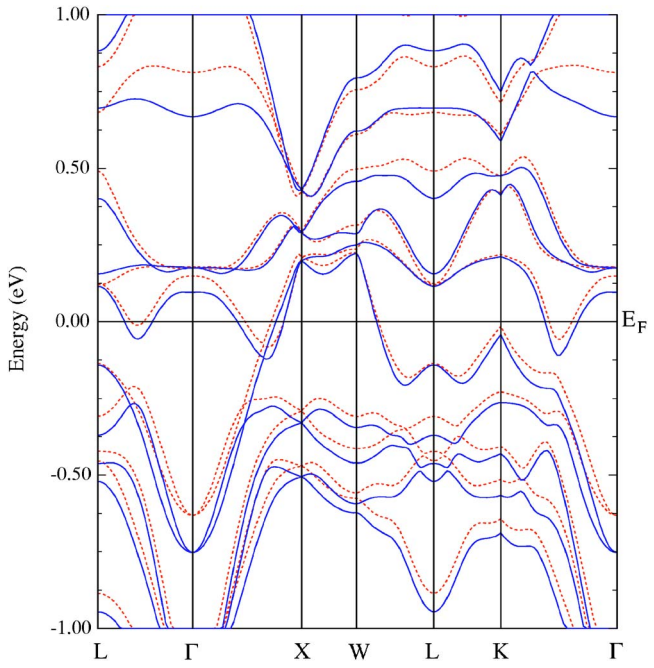

FIG. 3. (Color online) Band structure of $RbOs_2O_6$ for energies within 1 eV to E_F. Red-dotted curves: No pressure; solid-blue curves: Hydrostatic pressure such that $\Delta a/a=-2\%$. Clearly, the the van Hove singularity is pushed away from E_F.

TABLE III. $N(E_F)$ as a function of pressure, for KOs_2O_6 (in states/eV unit cell).

$\Delta V/V$	P (GPa)	$N(E_F)$
0%	0	9.64
0.5%	0.583	9.47
1%	1.166	9.33
3%	3.498	7.24

As one may expect, the above effects are reflected in the topology of the Fermi surface. This is of general interest because of its direct relation to electronic properties and the possible effect of the vHS on quasi-particle lifetimes. The Fermi surface consists of two closed electronlike sheets centered at the Γ point, and a third holelike sheet giving rise to a tubular network. These Fermi surface sheets are shown in Fig. 4, plotted for clarity in the reciprocal unit cell. The tubular network actually does not present any major difference among the compounds considered; as a typical example, we show the case of $CsOs_2O_6$ in Fig. 4(a). In contrast, the closed shells exhibit a clear difference near the midpoint of the Γ-L line, where the vHS is located. Indeed, in the case of $NaOs_2O_6$, in Fig. 4(b), the two shells show no narrowing of the distance at this point, while the narrowing is obvious in the case of $CsOs_2O_6$, as shown in Fig. 4(c). As discussed above, this is due to the closeness of the vHS to E_F in the latter case. The topology of the Fermi surface is also relevant to the superconducting gap. In relation to this, we note that the multiband character of the Fermi surface and the different symmetry of its sheets may be of significance to some of the experimental results on the β-pyrochlores. As pointed out above, Koda and co-workers[11] interpret their results on the linear field dependence of the penetration depth, λ, as suggesting a nonconventional pairing mechanism in KOs_2O_6, possibly mediated by magnetic fluctuations. However, in MgB_2, which is a phonon-mediated superconductor, λ also exhibits such a linear dependence on the applied field.[25] In the case of MgB_2 this arises because of its two-gap nature, which in turn is due to the particular character of its Fermi surface sheets, which we find akin to the present case to some extent.

B. Superconducting parameters

In the following, we examine the ability of a phonon-mediated pairing scenario to account for the experimental evidence, and, more particularly, the effects of alkali metal substitution and of pressure. To this end, we estimate the electron-phonon coupling constant λ_{ep} within the McMillan–Hopfield framework,[26,27] and the crude RMTA.[17,18] The spherically averaged Hopfield parameter can be written[28]

$$\eta_i = \sum_l M^2_{i_{l,l+1}} \frac{2l+2}{(2l+1)(2l+3)} \left[\frac{N_{i_l}(E_F) N_{i_{l+1}}(E_F)}{N(E_F)} \right], \quad (1)$$

where $N_{i_l}(E_F)$ is the l-angular momentum DOS projected on the muffin-tin sphere of atom i; $M_{i_{l,l+1}} = -\phi_{i_l}\phi_{i_{l+1}}[(D_{i_l}-l) \times (D_{i_{l+1}}+l+2)+(E_F-V_i)R_i^2]$ is an electron-phonon matrix element, in terms of the logarithmic derivatives (D_{i_l}) and the partial wave amplitudes (ϕ_{i_l}), both evaluated at E_F and at the muffin-tin radius (R_i); V_i is the one-electron potential at R_i. Then, we have $\lambda_{ep} = \Sigma_i \eta_i / \bar{M} \langle \omega_i^2 \rangle$, where $\bar{M}$ is the average

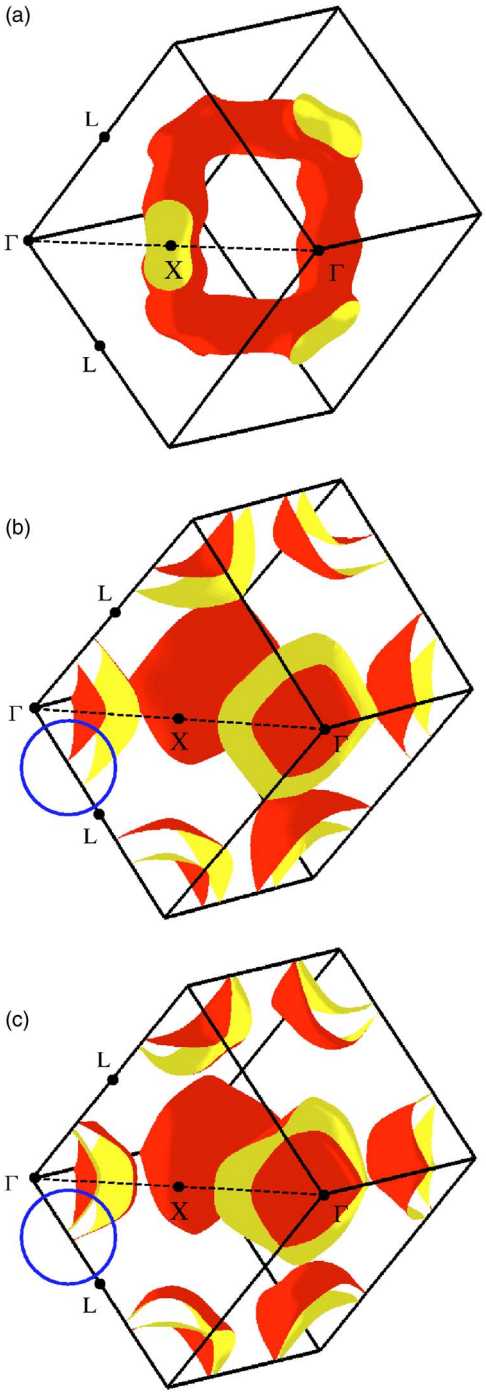

FIG. 4. (Color online) Fermi surface sheets of the β-pyrochlore Os oxides, plotted in the reciprocal unit cell. The "outer" surfaces of the sheets are colored red, while the "inner" ones are yellow. (a) The holelike tubular network, which does not change noticeably under change of the alkali metal. (b) The closed shell surfaces around the Γ point for $NaOs_2O_6$. No constriction along the Γ-L line is seen (cf. circle). (c) The constriction near the center of the Γ-L line, indicated by the circle, in the case of $CsOs_2O_6$ is clear.

TABLE IV. Electron-phonon coupling parameters of the Os oxide β-pyrochlores in the RMTA approximation, with $\Theta_D=285$ K. Hopfield parameters in eV/Å^2.

Compound	η_A	η_{Os}	η_O	λ_{ep}
$NaOs_2O_6$	3×10^{-6}	0.421	0.126	0.84
KOs_2O_6	1×10^{-4}	0.439	0.133	0.85
$RbOs_2O_6$	2×10^{-4}	0.449	0.137	0.80
$CsOs_2O_6$	5×10^{-4}	0.464	0.145	0.77

mass.[29] As is common, the average phonon frequency is estimated in terms of the Debye temperature as $\langle\omega^2\rangle^{1/2}=0.69\Theta_D$.

Regarding the Debye temperatures, there is unfortunately no experimental information for KOs_2O_6 and $CsOs_2O_6$. In the case of $RbOs_2O_6$, recent measurements suggest that the specific heat does not follow the usual $\sim T^3$ Debye model,[30] so that it is not clear what effective Θ_D is appropriate in our case. With this caveat, in our estimates, we use the value $\Theta_D=285$ K at $T=6$ K obtained if a parametrization of the heat capacity in terms of a T dependent Θ_D is enforced.[30] In Table IV, we present our results for the η_i and λ_{ep} for the different compounds.[31]

The critical temperature is subsequently calculated with the McMillan–Allen–Dynes equation[16,32]

$$T_c=\frac{\langle\omega^2\rangle^{1/2}}{1.2}\exp\left[-\frac{1.04(1+\lambda_{ep}+\mu_{sp})}{\lambda_{ep}-(\mu^*+\mu_{sp})(1+0.62\lambda_{ep})}\right], \quad (2)$$

where μ^* is the Coulomb pseudopotential and μ_{sp} is an effective electron-spin coupling constant. Note that, lacking the knowledge of the Eliashberg function $\alpha^2F(\omega)$, in lieu of the logarithmic average ω_{ln} we take the average phonon frequency, which we estimate in terms of Θ_D, as indicated above.[33] The Coulomb pseudopotential can be estimated through $\mu^*=0.26n(E_F)/[1+n(E_F)]$, where $n(E_F)$ is the DOS at E_F per eV and atom.[16] To estimate μ_{sp}, we use the expression derived by Doniach and Engelsberg $\mu_{sp}\simeq 3IN(E_F)\ln\{1+0.03IN(E_F)/[1-IN(E_F)]\}$.[19,34] The Stoner parameter in this expression, I, is calculated following the band formulation of Gunnarsson[35] and Brooks *et al.*[36] within spin-density-functional theory. More specifically, we have $I=\Sigma_i n_i I_i$, where n_i is the number of atoms of type i, and I_i the atomic Stoner parameter written as $I_i=\Sigma\hat{n}_{i_{ll'}}J_{i_{ll'}}$. Here $\hat{n}_{i_{ll'}}=N_{i_l}(E_F)N_{i_{l'}}(E_F)/N_i^2(E_F)$ and $J_{i_{ll'}}=\int dr|K(r)|\phi_{i_l}^2(r)\phi_{i_{l'}}^2(r)$ with, again, the partial wave amplitudes ϕ_{i_l} calculated at E_F. The exchange-correlation kernel K used is the one given by Gunnarsson.[35] In our case, the alkali atom contribution is completely negligible and only the diagonal $l=1$ term in O and the diagonal $l=2$ in Os contribute because of the dominance of the respective partial DOS at E_F (see, e.g., Ref. 36). We note that our calculations are done taking SOC into account.

Our results for the superconducting parameters, as well as for I and the Stoner enhancement factor $S=1/[1-IN(E_F)/2]$, are given in Table V. We note first that our calculated T_c (last column) follows well the experimental trend, although the range of the experimental T_c's is noticeably larger. Clearly, however, a more refined calculation of λ_{ep} based on, e.g., the frequency dependence of the Eliashberg function α^2F, can easily account for the difference of a fraction to a few K between our results and experiment seen in Table V. In this regard, Kuneš and co-workers[37] have found that the alkali ions in these materials possess a varying degree of anharmonicity in the potential, which would add to the difference in their T_c's. Second, we note the significant role of spin fluctuations. Indeed, with $\mu_{sp}=0$ the predicted T_c (given as T_c') is $\sim$72% (KOs_2O_6) to $\sim$144% ($CsOs_2O_6$) higher. Thus, although the calculated Stoner enhancement factors ($2<S<3$) indicate that these systems are not close to a ferromagnetic instability, they are sufficient to produce a significant electron-spin coupling.

Finally, we have calculated the superconducting parameters of KOs_2O_6 (again with $\Theta_D=285$ K) under the simulated effect of pressure, to study the initial change of T_c with pressure. We have considered pressures up to 1.166 GPa, which is of the order of the pressures used in the experimental report by Muramatsu *et al.*[13] Our results are given in Table VI. As in experiment,[12,13] we see that T_c increases with pressure, although λ_{ep} decreases. The main reason is that both μ^* and μ_{sp} also decrease, and more importantly the latter than the former. Hence, the initial increase of T_c with pressure appears to be due mainly to a decrease of spin fluctuations, driven by the decrease of $N(E_F)$ (the Stoner parameter I is almost unchanged). Comparing our results with the ratio $T_c/T_c^0=1.04$ found at 0.56 GPa by Muramatsu and collaborators,[13] we see that the change in T_c is of the same order and is essentially accounted for. Indeed, if the main cause were to be phononic, i.e., a change in Θ_D, the latter would have to decrease with pressure, contrary to any likelihood.[38] Again, we surmise that a more refined calculation can readily account for the somewhat steeper initial in-

TABLE V. Superconducting parameters of the Os oxide β-pyrochlores. μ^* is the Coulomb pseudopotential; I and S are the Stoner parameter and susceptibility enhancement factor, respectively, and μ_{sp} is the electron-spin coupling constant; T_c' denotes the calculated critical temperature with $\mu_{sp}=0$.

Compound	μ^*	I (eV)	S	μ_{sp}	T_c' (K)	T_c^{exp} (K)	T_c (K)
$NaOs_2O_6$	0.088	0.1166	2.14	0.054	10.9	—	7.0
KOs_2O_6	0.091	0.1166	2.28	0.064	11.0	9.6	6.4
$RbOs_2O_6$	0.093	0.1162	2.37	0.070	9.7	6.3	5.0
$CsOs_2O_6$	0.096	0.1155	2.57	0.084	8.8	3.3	3.6

TABLE VI. Superconducting parameters as a function of pressure for KOs_2O_6 (Θ_D=285 K). T_c^0 corresponds to 0 pressure.

Pressure (GPa)	μ^*	S	μ_{sp}	λ_{ep}	T_c/T_c^0
0	0.091	2.28	0.064	0.852	1
0.583	0.090	2.23	0.060	0.845	1.03
1.166	0.089	2.19	0.057	0.841	1.05

crease of T_c observed. In their experimental study of the change of T_c with pressure in the case of $RbOs_2O_6$, Khasanov and co-workers[12] had already concluded that the observed positive slope at low pressures must arise mainly from electronic contributions, as opposed to phononic ones, although the mechanism behind the effect was still an open question.

We note that the very recent report by Muramatsu and collaborators[39] shows that in the present family of superconductors, after reaching a maximum value, with increasing pressure T_c will gradually decrease, falling below its ambient pressure value, until superconductivity is eventually suppressed. To make predictions of T_c at those high pressures, however, it would be necessary to have a minimum information on the phonon spectra and how they are affected by pressure. We do not know what would be a sensible value of Θ_D to make such estimates of T_c within our approach. However, we can try to understand what happens as follows. If the Grüneisen parameter for KOs_2O_6 is around 1.8, which is a rough average for most substances,[40] then for a pressure P=3.5 GPa (corresponding to $-\Delta V/V \simeq 3\%$), $\Theta_D \simeq 301$ K. The calculated superconducting parameters (μ^*=0.085, μ_{sp} =0.048, and λ_{ep}=0.738) then would lead to $T_c/T_c^0 \simeq 0.88$ (against $\simeq$0.66 in experiment). This result suggests that the decrease of T_c at higher pressures could be understood as reflecting the fact that, in that regime, the phononic properties become dominant.

It is remarkable, given the approximate nature of our estimate of λ_{ep} and T_c, that our results account rather well for the behavior of T_c under substitution of the alkali metal and under applied pressure. We believe this brings strong support for the phonon-mediated pairing scenario. To understand more fully the properties of the β-pyrochlore Os oxides, however, further investigation will be required, experimentally and theoretically. For instance, the different nuclear spin-lattice relaxation rates of the alkali ions in KOs_2O_6 and $RbOs_2O_6$ remain to be clarified. This could be partly due to the rapid variation of the DOS close to E_F. Indeed, Fig. 2 shows that $N(E_F)$ can change by as much as 50% within an energy range of ±25 meV (more so the heavier the alkali ion). A further contribution may come from the changing character of the alkali atom DOS at E_F. We find that its s character falls from 73% in $NaOs_2O_6$, to 11% in $CsOs_2O_6$, passing by 31% in KOs_2O_6 and 23% in $RbOs_2O_6$ (at the same time its p character rises from 16% in $NaOs_2O_6$, to 55% in $CsOs_2O_6$, passing by 31% in KOs_2O_6 and 38% in $RbOs_2O_6$).

Furthermore, the origin of the unusual behavior of the resistivity in KOs_2O_6 at low T is also not understood, nor is the rather large specific heat mass enhancements γ_{exp}/γ_b in all these materials. The electron-phonon and electron-spin coupling constants obtained above are clearly insufficient to account for the observed enhancements of 3–4. It is possible that the vHS near E_F and the nesting exhibited by the Fermi surface[41] contribute to both the resistivity and the specific heat. The observed enhancements suggest, in our view, that the unusual non-Debye behavior at low temperature of the specific heat mentioned above is a generic property.

ACKNOWLEDGMENTS

We thank Lin-Hui Ye, S. H. Rhim, J. B. Ketterson, and W. Halperin for helpful discussions. We are also grateful to B. Barbiellini and G. Grimvall for their suggestions and to B. Battlogg and M. Brühwiler for sharing data with us prior to publication. This work was supported by the Department of Energy (under Grant No. DE-FG02-88ER 45372/A021 and a computer time grant at the National Energy Research Scientific Computing Center).

[1] S. Yonezawa, Y. Muraoka, Y. Matsushita, and Z. Hiroi, J. Phys.: Condens. Matter **16**, L9 (2004).
[2] S. Yonezawa, Y. Muraoka, Y. Matsushita, and Z. Hiroi, J. Phys. Soc. Jpn. **73**, 819 (2004).
[3] S. Yonezawa, Y. Muraoka, and Z. Hiroi, J. Phys. Soc. Jpn. **73**, 1655 (2004).
[4] Z. Hiroi, S. Yonezawa, and Y. Muraoka, J. Phys. Soc. Jpn. **73**, 1651 (2004).
[5] M. Hanawa, Y. Muraoka, T. Tayama, T. Sakakibara, J. Yamaura, and Z. Hiroi, Phys. Rev. Lett. **87**, 187001 (2001).
[6] R. Jin, J. He, S. McCall, C. S. Alexander, F. Drymiotis, and D. Mandrus, Phys. Rev. B **64**, 180503(R) (2001).
[7] D. Mandrus, J. R. Thompson, R. Gaal, L. Forro, J. C. Bryan, B. C. Chakoumakos, L. M. Woods, B. C. Sales, R. S. Fishman, and V. Keppens, Phys. Rev. B **63**, 195104 (2001).
[8] M. Brühwiler, S. M. Kazakov, N. D. Zhigadlo, J. Karpinski, and B. Batlogg, Phys. Rev. B **70**, 020503(R) (2004).
[9] K. Magishi, J. L. Gavilano, B. Pedrini, J. Hinderer, M. Weller, H. R. Ott, S. M. Kazakov, and J. Karpinski, Phys. Rev. B **71**, 024524 (2005).
[10] K. Arai, J. Kikuchi, K. Kodama, M. Takigawa, S. Yonezawa, Y. Muraoka, and Z. Hiroi, cond-mat/0411460.
[11] A. Koda, W. Higemoto, K. Ohishi, S. R. Saha, and R. Kadono, cond-mat/0402400.
[12] R. Khasanov, D. G. Eshchenko, J. Karpinski, S. M. Kazakov, N. D. Zhigadlo, R. Brütsch, D. Gavillet, D. DiCastro, A. Shengelaya, F. La Mattina, A. Maisuradze, C. Baines, and H. Keller, Phys. Rev. Lett. **93**, 157004 (2004).
[13] T. Muramatsu, S. Yonezawa, Y. Muraoka, and Z. Hiroi, J. Phys. Soc. Jpn. **73**, 2912 (2004).
[14] After the submission of this manuscript, Muramatsu and coworkers reported new high pressure measurements (pressures up

to 10 GPa), showing that T_c follows a similar trend in all three compounds with A=K, Rb, and Cs, and that under appropriate normalization the plots of T_c versus P appear to fall under a same universal curve. See Ref. 39.

[15] R. Saniz, J. E. Medvedeva, Lin-Hui Ye, T. Shishidou, and A. J. Freeman, Phys. Rev. B **70**, 100505(R) (2004).

[16] K. Bennemann and J. Garland, AIP Conf. Proc. **4**, 103 (1972).

[17] G. P. Gaspari and B. L. Gyorffy, Phys. Rev. Lett. **28**, 801 (1972).

[18] D. G. Pettifor, J. Phys. F: Met. Phys. **7**, 1009 (1977).

[19] S. Doniach and S. Engelsberg, Phys. Rev. Lett. **17**, 750 (1966).

[20] E. Wimmer, H. Krakauer, M. Weinert, and A. J. Freeman, Phys. Rev. B **24**, 864 (1981); M. Weinert, E. Wimmer, and A. J. Freeman, *ibid.* **26**, 4571 (1982); H. J. F. Jansen and A. J. Freeman, *ibid.* **30**, 561 (1984).

[21] J. P. Perdew, K. Burke, and M. Ernzerhof, Phys. Rev. Lett. **77**, 3865 (1996).

[22] M. Brühwiler, S. M. Kazakov, J. Karpinski, and B. Batlogg, cond-mat/0502125.

[23] Z. Hiroi, S. Yonezawa, J.-I. Yamaura, T. Muramatsu, and Y. Muraoka, cond-mat/0502043.

[24] This result calls for similar measurements on the other Os oxide β-pyrochlores, not least because, in addition, a second peak is observed in the C/T curve, below the superconducting T_c, which could indicate a further first-order or λ-type phase transition.

[25] K. Ohishi, T. Muranaka, J. Akimitsu, A. Koda, W. Higemoto, and R. Kadono, J. Phys. Soc. Jpn. **72**, 29 (2003).

[26] W. L. McMillan, Phys. Rev. **167**, 331 (1968).

[27] J. J. Hopfield, Phys. Rev. **186**, 443 (1969).

[28] H. L. Skriver and I. Mertig, Phys. Rev. B **32**, 4431 (1985).

[29] There are several formulas to calculate λ_{ep} in the case of compounds [see M.-C. Huang, H. J. F. Jansen, and A. J. Freeman, Phys. Rev. B **37**, 3489 (1988), and references therein]. In our case, we think it is more sensible to take the average mass $\bar{M}$ instead of the atomic masses M_i, because it is known that the latter overweights the contribution of light atoms like O.

[30] M. Brühwiler and B. Batlogg (private communication).

[31] An estimate of a zero temperature Θ_D^e from the elastic constants of these materials shows that it decreases with increasing size of A and one can expect Θ_D to follow the same trend. However, it is known that Θ_D generally decreases quadratically with temperature at low temperatures (see, e.g., G. Grimvall, *Thermophysical properties of materials* (Elsevier, Amsterdam, 1999), p. 97), so that the observed decrease of T_c with the size of A is expected to result in Θ_D at T_c moving upward, tending to compensate the first effect. Thus, we use the same Θ_D for all the compounds in our calculations.

[32] P. B. Allen and R. C. Dynes, Phys. Rev. B **12**, 905 (1975).

[33] It is difficult to know beforehand whether the correction of $\omega_{\ln}$ over $\langle\omega^2\rangle^{1/2}$ is small or not for a given compound. However, the account presented here of the trends observed in experiment allows us *a posteriori* to expect that the correction will not be too large and that the physical content of our description will be preserved.

[34] As Doniach and Engelsberg (Ref. 19), we use a momentum cutoff p/p_F=0.6

[35] O. Gunnarsson, J. Phys. F: Met. Phys. **6**, 587 (1976).

[36] M. S. S. Brooks, O. Ericksson, and B. Johansson, Phys. Scr. **35**, 52 (1987).

[37] J. Kuneš, T. Jeong, and W. E. Pickett, Phys. Rev. B **70**, 174510 (2004).

[38] As noted above (cf. Ref. 31), Θ_D^e increases with decreasing lattice constant (positive chemical pressure), thus indicating a positive Grüneisen constant.

[39] T. Muramatsu, N. Takeshita, C. Terakura, H. Takagi, Y. Tokura, S. Yonezawa, Y. Muraoka, and Z. Hiroi, cond-mat/0502490.

[40] J. A. Gschneider, Jr., in *Solid State Physics*, edited by F. Seitz and D. Turnbull (Academic, New York, 1964), Vol. 64, p. 275.

[41] In Ref. 37, a calculation of the bare band susceptibility along the Γ-K direction is reported for KOs_2O_6. Although it appears not to suggest electronic instabilities, it does show clear nesting effects. We note that the constriction between the two closed Fermi surfaces discussed above may have effects on the nesting; in particular, it may degrade any nesting along the [111] direction in the case of the heavier alkali metals.